Single-domain Switching Dynamics in BEOL Nanoscale Ferroelectric Field-effect Transistors

Yanjie Shao[1]*, Minsoo Kim[1,2], John C.-C. Huang[1], Dimitri A. Antoniadis[1], and Jesús A. del Alamo[1]
[1]Microsystems Technology Laboratories, MIT, Cambridge, MA 02139, USA, *email: shaoyj@mit.edu
[2]DRAM Product Engineering Team, Samsung Electronics, Hwaseong 18448, South Korea

***Abstract*—**We study polarization switching dynamics in back-end-of-the-line (BEOL) oxide-channel ferroelectric field-effect transistors (FE-FETs) based on 10 nm thick FE-$HfZrO_2$ (FE-HZO). We demonstrate single-domain switching in nanoscale devices at a voltage amplitude < 1.8 V and pulse width < 10 ns. Leveraging this device platform, we have studied FE polarization accumulation and relaxation in response to a pulse train in wide as well as very narrow devices where we can observe single-domain switching. Remarkably, polarization accumulation and relaxation dynamics is virtually identical in both types of devices, suggesting a large stochasticity in single domain switching which dominates that of a large domain ensemble.

I. Introduction

FE-HZO has emerged as a key enabler for future embedded non-volatile memory (eNVM) [1], ranging from FE dynamic random-access memory (FE-DRAM) to FE tunnel junction (FTJ) and to FE-FET [2]. Typical FE-HZO films are polycrystalline with an average grain size of ~20-30 nm [3], leading to FE domains of a similar size. As the dimensions of device active region approach the nanometer regime in high-density memory arrays, it is expected that few- or single-domain behavior would eventually dominate polarization switching characteristics [4]. FE domain dynamics directly affect the switching speed, operating voltage and memory reliability of HZO-based eNVM devices, and thus a detailed understanding of FE polarization reversal kinetics is essential.

While one-shot polarization switching schemes (i.e., applying a single pulse with certain Program voltage, V_P and pulse width, t_{pulse}) have been extensively evaluated, the cumulative switching behavior (i.e., applying a pulse train with certain delay time between pulses, t_{delay}) remains controversial [5-9]. Yet, this operating mode has high relevance for write/read disturbs in memory arrays, gradual conductance programming in analog crossbar arrays, and leaky behavior in spiking neural networks, among others.

Recently, we have demonstrated discrete FE polarization switching in scaled FE-FETs based on an amorphous oxide-semiconductor (AOS) channel [10,11]. In this paper, we leverage this unique platform to study polarization switching dynamics in short-channel FE-FETs with either a large width, encompassing a large number of active domains, or a nanoscale width, with few active domains. We first characterize single-shot domain switching behavior and demonstrate fast switching (< 10 ns) at a low voltage (< 1.8 V). We then investigate cumulative switching characteristics and observe a surprisingly broad stochasticity even in a single domain. Strikingly, it appears that single-domain stochasticity of polarization accumulation and relaxation dominates large-area ensemble behavior. Finally, we find that the accumulation of FE polarization in a single domain becomes harder as the device ages, providing new insights into FE device fatigue.

II. Device Fabrication

Device schematic is shown in **Fig. 1**. Details of device fabrication can be found in [11]. Our process is BEOL-compatible with a 400 °C thermal budget. To evaluate domain-level FE switching dynamics, we designed and fabricated devices with a highly scaled active region with dimensions down to ~30 nm in both channel width (W) and channel length (L_{ch}) (**Fig. 2**). We also characterized the surface morphology of the FE-HZO film (**Fig. 3**) fabricated at the same time with FE-FETs and following the same activation process. An average grain size of ~18-20 nm was obtained.

III. Memory Characteristics of BEOL FE-FETs

Bi-directional DC transfer characteristics in both log and linear scales of a device with W/L_{ch} = 35/30 nm are shown in **Fig. 4**. A single and sharp FE switching event is observed at both positive and negative V_{gs} regimes indicated by the red arrows, suggesting a single active domain in this device. With an increased device active area (W/L_{ch} = 50/40 nm), switching of two domains is observed, as shown in **Fig. 5**.

Applying the pulse scheme in **Fig. 6(a)** to a W/L_{ch} = 40/40 nm device, two *and only two* stable conductance (G) states were repeatedly observed at a short t_{pulse} = 20 ns [**Figs. 6(c)** and **(d)**]. Schematic transfer characteristics of the device and the corresponding domain polarization directions in the two states are sketched in **Fig. 6(b)**.

We have carried out detailed studies of single-shot domain switching dynamics in short-L_{ch} devices with either tiny or wide W. Before each Erase (Program) measurement, a full Program (Erase) pulse was applied to initialize the device to its lowest (highest) threshold voltage (V_t) state. After that, we applied a single Erase (Program) pulse with varying pulse amplitude and pulse width. **Figs. 7(a)** and **8(a)** show detailed pulse schemes. Abrupt G switching is observed in scaled-footprint devices with few domains both in Erase and Program experiments [**Figs. 7(b)** and **8(b),** respectively], while gradual G switching is observed in wide devices with a large domain ensemble [**Figs. 7(c)** and **8(c)**]. In both Erase and Program operations in all devices, a larger voltage amplitude results in exponential decrease of the t_{pulse} required to switch the device to the same G level [**Figs. 7(b)-(c)** and **8(b)-(c)**]. Our experiments also reveal that in our BEOL AOS FE-FETs domain switching in both directions can be completed with a voltage amplitude < 1.8 V (corresponding to an electric field strength of 1.8 MV/cm) and a t_{pulse} < 10 ns (instrumentation limit) [**Figs. 7(b)** and **8(b)**]. These metrics are comparable to a recent demonstration with a similar device architecture [12]. It is also worth noting that the switching speed in our devices is several orders of magnitude faster than state-of-the-art Si FE-FETs with an identical FE-dielectric thickness at any given operating voltage [13]. This is ascribed to the potential absence of an interfacial layer between channel and FE-dielectric resulting in a lower equivalent oxide thickness.

IV. Accumulation and Relaxation of FE Polarization down to Single Domain

We have further performed systematic cumulative switching experiments in our FE-FETs. The pulse scheme is shown in **Fig. 9**. A full Erase pulse was applied before each measurement. A pulse train was then applied with t_{pulse} = 20 ns and varying V_P, number of pulses (N), and t_{delay} between pulses. Pulse rise and fall times were both 8 ns, the instrumentation limit. For each Read, we sampled the channel G ten times at V_{ds} = 0.05 V and V_{gs} = -0.2 V and derived an average G value.

Figs. 10(a)-(b) show G in a wide and short device as a function of N in two different experiments that investigate cumulative switching. Each data point represents a unique experiment on the same device. Setting t_{delay} = 0, as V_P increases from 1.9 to 3.5 V, a shorter pulse train is required for G to reach its final value [**Fig. 10(a)**]. Separately, fixing V_P = 2 V, we investigated cumulative switching by examining the impact of t_{delay} [**Fig. 10(b)**]. For t_{delay} < ~10 µs, polarization accumulation is clearly visible in an increasing G with N. For t_{delay} greater than ~10 µs, G reaches steady state virtually after the very first pulse suggesting that no polarization accumulation is taking place. In the intermediate regime, as t_{delay} increases beyond ~10 ns, a lower ultimate value of steady-state G is achieved. These results are consistent with earlier observations of polarization switching in FE-capacitors and FE-FETs [6,9]. The trend of steady-state G (average G over N = 16-20) versus t_{delay} of **Fig. 10(c)** indicates a dynamic competition between polarization accumulation and relaxation in the range ~10 ns < t_{delay} < ~10 µs.

We have performed a similar study on a narrow and short device characterized by three G states, corresponding to two active domains. In this case, the switching behavior is very sensitive to V_P [**Fig. 11(a)**]. With t_{delay} = 0, when V_P is large enough (≥ 2 V), a single pulse consistently switches both domains. In contrast, 1.65-V pulse trains with N up to 10 only manage to switch the domain with a lower coercive field (denoted as domain #1) and in an inconsistent manner. This reveals considerable stochasticity of domain #1 polarization accumulation at 1.65 V. At an intermediate V_P, both domains switch sequentially [**Fig. 11(a)**]. Specifically, at V_P = 1.8 V, domain #1 is switched every time with a single pulse, while 3-5 consecutive pulses are required to switch domain #2 (the domain with a higher coercive field) indicating additional stochasticity in the polarization switching of domain #2 [**Fig. 11(b)**]. Schematic FE polarization state in each domain for each G state is indicated on the right side of **Fig. 11(b)**.

To investigate cumulative switching behavior in a single domain (domain #2 in this case), we fixed V_P = 1.8 V, N = 10, and carried out repeated measurements with different t_{delay}. **Fig. 12** shows exemplar results at three t_{delay} values. We find that the switching probability (S_p) of domain #2 decreases as t_{delay} increases. The stochasticity of FE domain polarization accumulation and relaxation versus t_{delay} is graphed in **Fig. 13.** For each data point, at least 10 repeated experiments were carried out. A striking stochasticity of single domain accumulation and relaxation for t_{delay} between ~10 ns and ~10 µs emerges, which is consistent with that observed in the wide device [**Fig. 10(c)**]. This surprising result suggests that single-domain stochasticity dominates large-area ensemble behavior.

Repeated switching events resulted in device fatigue. After ~10^5 total polarization switching cycles, domain #1 became pinned in the up-polarization state [10], i.e., channel G was stuck in the middle state even after a long Erase pulse (~1 s) with large pulse amplitude (-5 V). Under these conditions, we studied domain #2 polarization accumulation behavior again following similar pulse train measurements as in **Fig. 11.** The switching of domain #2 was again found to be extremely sensitive to V_P [**Fig. 14(a)**]. At V_P = 1.8 V and t_{delay} = 0, 2-5 consecutive pulses were required to switch domain #2 [**Fig. 14(b)**], similar to the results in **Fig. 11(b)**. In subsequent experiments examining the impact of t_{delay}, S_p was found to change over a narrower range from ~20 ns to ~1 µs (**Fig. 15**) with respect to the results of **Fig. 13** in the same device. This indicates that FE polarization accumulation in a single domain becomes harder as FE fatigue settles in.

In the framework of the Nucleation-Limited Switching (NLS) theory, polarization reversal under an external field is limited by the incubation of critical-size reversed-polarity seeds which then rapidly expand to form a reversed domain. The application of this model to polarization accumulation and relaxation experiments suggests the existence of a relaxation process in the absence of an external electric field that delays as in [14] or even prohibits seed maturation. Separately, Saha *et al.* has postulated domain wall (DW) instability in the absence of an applied electric field as such a relaxation process [15]. DW instability is likely to be very sensitive to factors such as charge trapping, electric field fluctuations, ionic movement and others, leading to large switching stochasticity at the single domain level. This could also come to dominate stochasticity of a multi-grain ensemble, consistent with our experiments (**Fig. 16**).

Our work reveals a large stochasticity for single-domain switching under sub-coercive-field pulses. On the other hand, under large enough voltage, a single domain responds in a deterministic manner [**Figs. 6(c)-(d)**].

V. Conclusions

This work leverages a unique BEOL nanoscale FE-memory platform in the study of polarization switching dynamics of FE-HZO. We have investigated the switching behavior of a single FE domain and observed a wide stochasticity in the balance between polarization accumulation and relaxation in response to a pulse train. Remarkably, a wide device encompassing a large ensemble of domains displays virtually identical accumulation/relaxation dynamics.

Acknowledgment

This work was supported by SRC (#3140.001) and Intel Corporation through MIT AI HW Program. Device fabrication was carried out at MTL and MIT.nano facilities of MIT.

References

[1] T. S. Böscke et al., *APL* 99, 102903, 2011. [2] T. Mikolajick et al., *TED*, 67, 1434, 2020. [3] M. Lederer et al., *APL*, 115, 222902, 2019. [4] H. Mulaosmanovic et al., *ACS AMI*, 9, 3792, 2017. [5] H. Mulaosmanovic et al., *ACS AMI*, 10, 23997, 2018. [6] C. Alessandri et al., *TED*, 66, 3527, 2019. [7] H. Mulaosmanovic et al., *TED*, 67, 5804, 2020. [8] M. Hoffmann et al., *EDL*, 43, 2097, 2022. [9] M. Otomo et al., *VLSI*, T15.2.1, 2024. [10] Y. Shao et al., *Nano Lett.*, 25, 3173, 2025. [11] Y. Shao et al., *IEDM*, 2024. [12] S. G. Kirtania et al., *IEDM*, 2024. [13] M. M. Dahan et al., *Nano Lett.*, 23, 1395, 2023. [14] D. A. Antoniadis et al., *TED*, 69, 395, 2022. [15] A. K. Saha et al., *APL*, 114, 202903, 2019.

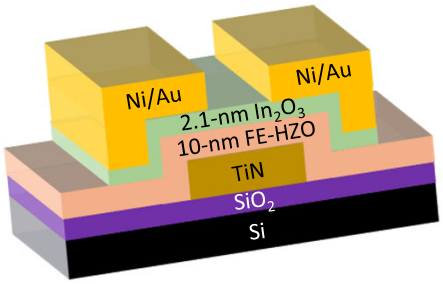

Fig. 1. Schematic BEOL FE-FET structure with PEALD In_2O_3 channel. 10 nm FE-HZO is used as gate dielectric.

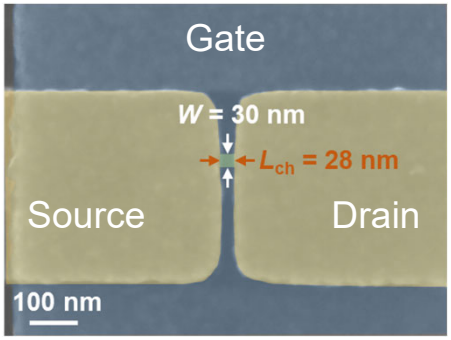

Fig. 2. False-colored SEM image of FE-FET showing highly-scaled active area with W = 30 nm and L_{ch} = 28 nm.

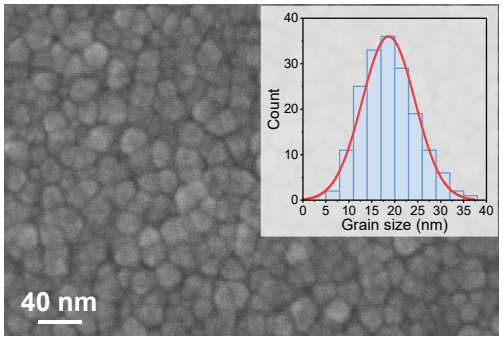

Fig. 3. Top-down SEM image of polycrystalline HZO film on TiN, prepared alongside FE-FET fabrication. Inset: HZO grain size distribution.

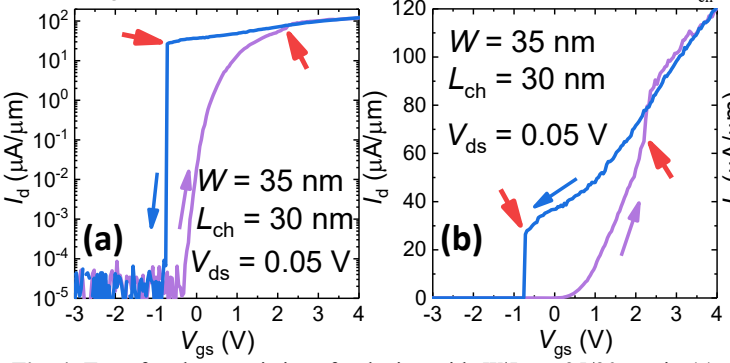

Fig. 4. Transfer characteristics of a device with W/L_{ch} = 35/30 nm in (a) log scale and (b) linear scale. Red arrows depict discrete FE polarization switching events. This device shows single domain switching behavior.

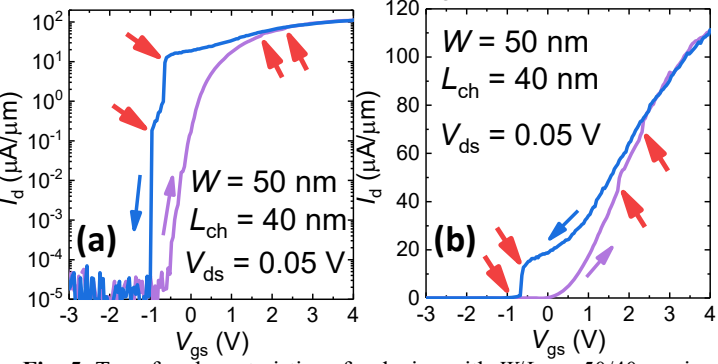

Fig. 5. Transfer characteristics of a device with W/L_{ch} = 50/40 nm in (a) log scale and (b) linear scale, showing two discrete switching events as depicted by red arrows.

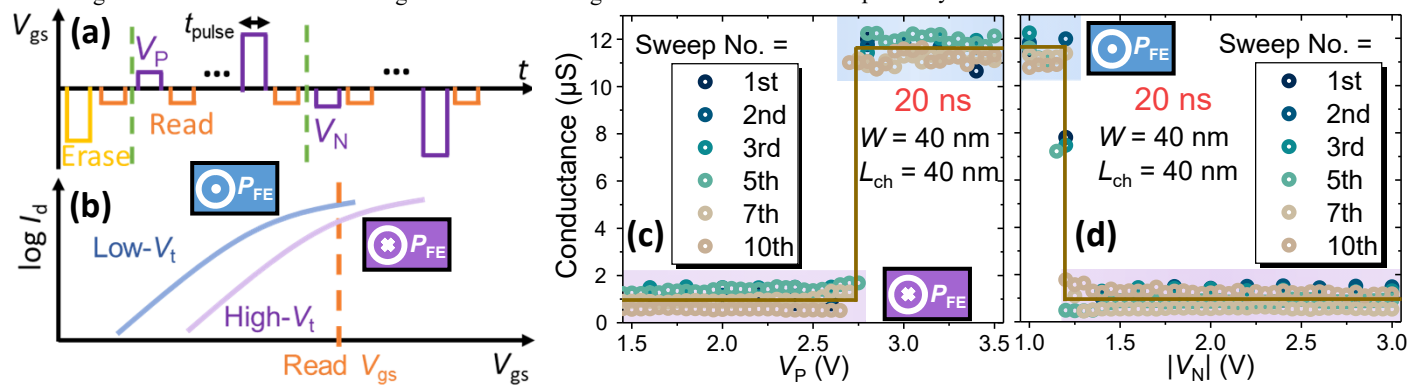

Fig. 6. (a) Pulse scheme applied with t_{pulse} = 20 ns. (b) Schematic subthreshold behavior for a single-domain device. The polarization direction of the domain from a top-down view is also schematically shown. (c),(d) Channel conductance read at a constant V_{gs} = -0.2 V from a FE-FET with W/L_{ch} = 40/40 nm versus (c) V_P and (d) $|V_N|$ pulses, showing single-domain FE switching.

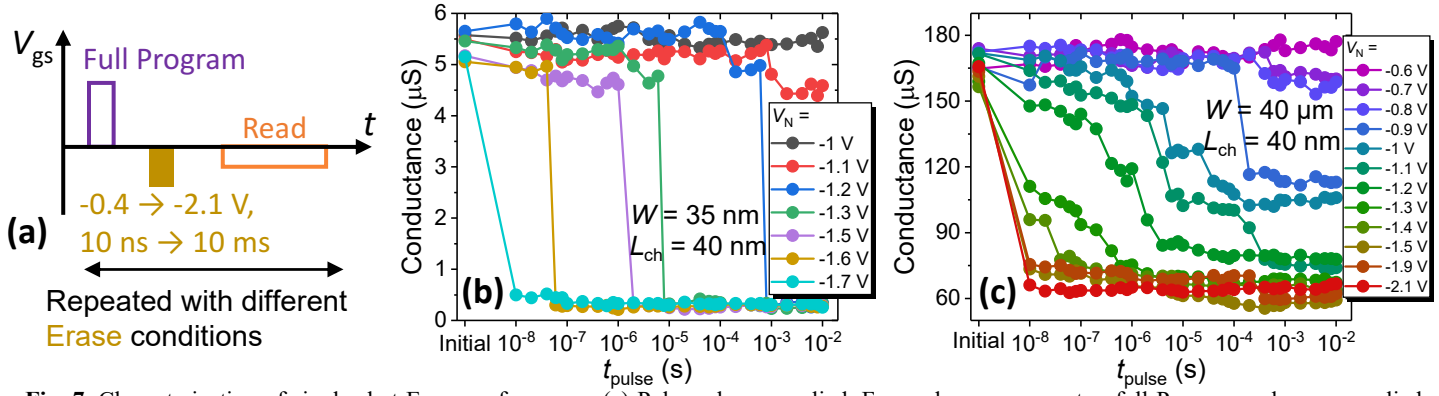

Fig. 7. Characterization of single-shot Erase performance. (a) Pulse scheme applied. For each measurement, a full Program pulse was applied first, followed by different Erase conditions. (b),(c) Channel conductance read at a constant V_{gs} = -0.2 V as function of t_{pulse} at different V_N levels from devices with (b) a nanoscale footprint featuring W/L_{ch} = 35/40 nm and (c) a wide channel featuring W/L_{ch} = 40 μm/40 nm.

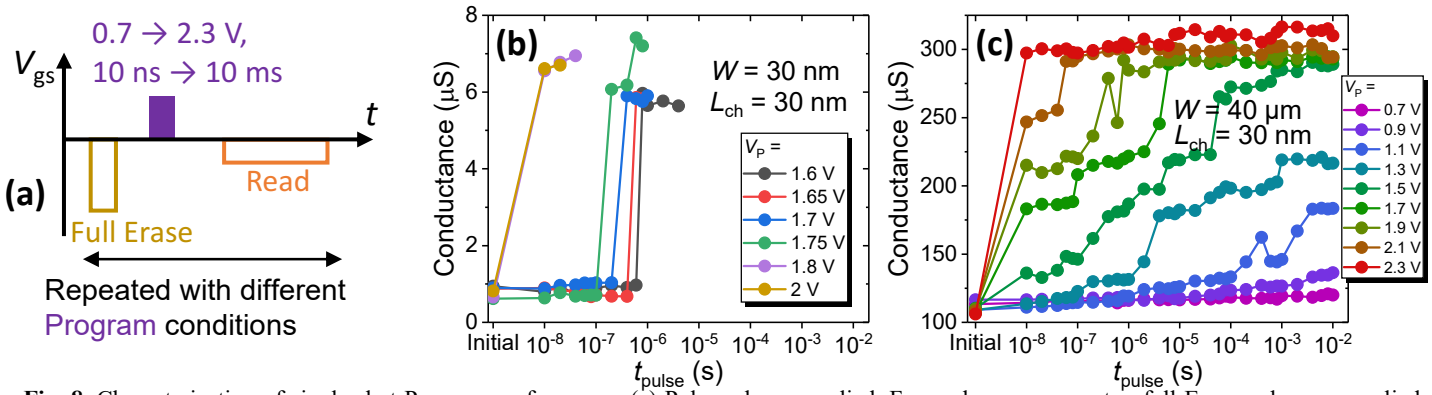

Fig. 8. Characterization of single-shot Program performance. (a) Pulse scheme applied. For each measurement, a full Erase pulse was applied first, followed by different Program conditions. (b),(c) Channel conductance read at a constant V_{gs} = -0.2 V as function of t_{pulse} at different V_P levels from devices with (b) a nanoscale footprint featuring W/L_{ch} = 30/30 nm and (c) a wide channel featuring W/L_{ch} = 40 μm/30 nm.

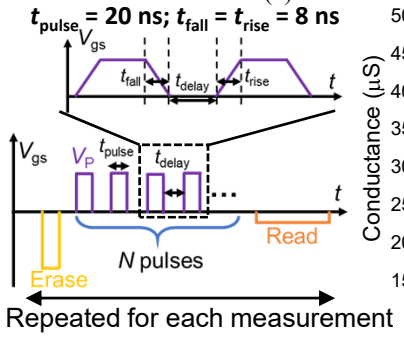

Fig. 9, Pulse scheme for accumulative FE switching study. For each measurement, a full Erase pulse was applied first.

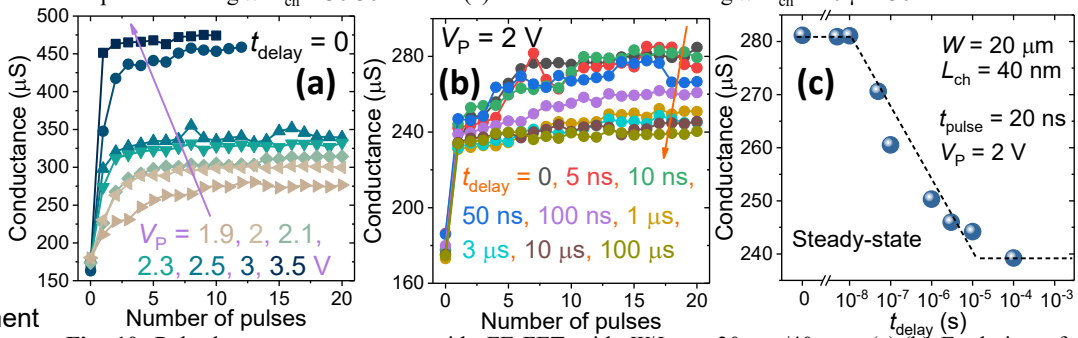

Fig. 10. Pulsed measurements on a wide FE-FET with W/L_{ch} = 20 μm/40 nm. (a),(b) Evolution of channel conductance versus number of pulses with (a) varying V_P at t_{delay} = 0 and (b) varying t_{delay} at V_P = 2 V, using the scheme in **Fig. 9**. (c) Final steady-state conductance versus t_{delay}.

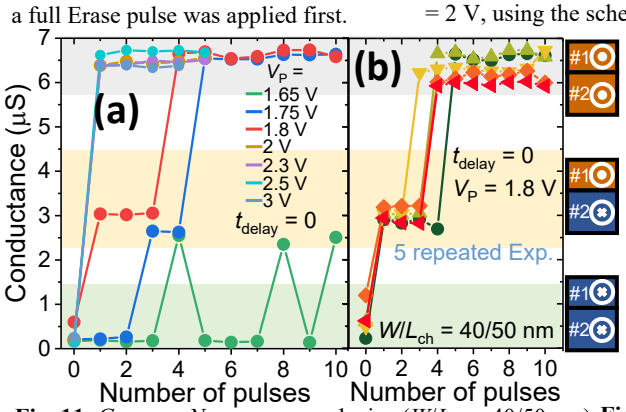

Fig. 11. G versus N on a narrow device (W/L_{ch} = 40/50 nm) with (a) varying V_P at t_{delay} = 0 and (b) repeated experiments at V_P = 1.8 V and t_{delay} = 0. Two domains are active.

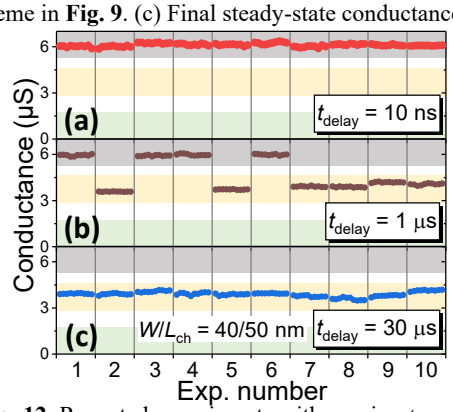

Fig. 12. Repeated experiments with varying t_{delay} at N = 10 and V_P = 1.8 V on the narrow device. Each experiment include 10 Read samples.

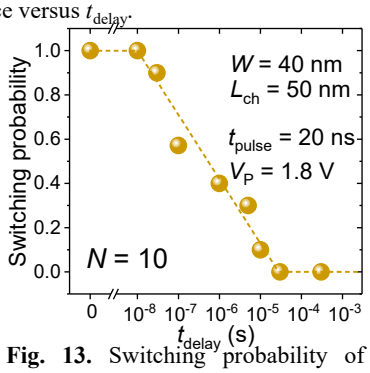

Fig. 13. Switching probability of domain #2 versus t_{delay} at V_P = 1.8 V. Each data point represents at least 10 repeated experiments. The dashed line is a guide for the eyes.

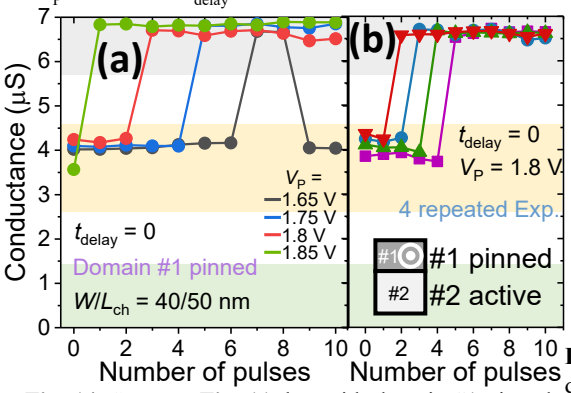

Fig. 14. Same as **Fig. 11**, but with domain #1 pinned in the low-V_t state after ~10^5 total switching cycles.

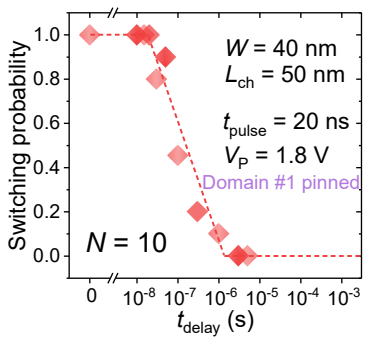

Fig. 15. Same as **Fig. 13**, but with domain #1 pinned. A steeper decrease of switching probability versus t_{delay} is observed when compared to **Fig. 13**.

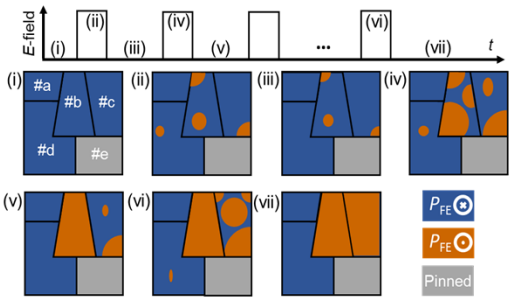

Fig. 16. Schematic FE polarization accumulation and relaxation under a pulse train. When reversed-polarity seeds do not attain critical size to switch the whole domain, the absence of E-field between pulses prevents seed maturation.